

X-Ray Lines from Hot Flows around White Dwarfs. Application to SS Cygni.

Kristen Menou,¹

Princeton University, Department of Astrophysical Sciences, Princeton NJ 08544, USA,
kristen@astro.princeton.edu

Rosalba Perna² and John C. Raymond

Harvard-Smithsonian Center for Astrophysics, 60 Garden Street, Cambridge MA 02138, USA,
rperna@cfa.harvard.edu, jraymond@cfa.harvard.edu

ABSTRACT

Rather than accreting via a disk, some White Dwarfs (WDs) in quiescent Dwarf Novae (DN) could accrete via an Advection-Dominated Accretion Flow (ADAF) possibly responsible for the X-ray Bremsstrahlung emission observed. Such a hot accretion flow is also expected to produce characteristic thermal line emission. Using SS Cyg as a specific example, we show that knowing *a priori* the inclination and the WD mass in quiescent DN makes X-ray line diagnostics powerful probes of the flow structure in these systems. Current X-ray instruments can discriminate, from their width, between lines emitted from a flow with a Keplerian rotation rate and those emitted at a substantially sub-Keplerian rate. This could be used to observationally test the property of energy advection, which is at the origin of the partial radial pressure support by the hot gas and the sub-Keplerian rotation rate in an ADAF.

Subject headings: X-ray: stars – binaries: close – accretion, accretion disks – stars: white dwarfs

1. Introduction

Dwarf novae (DN) are members of the class of Cataclysmic Variables (CVs), which are binary stars composed of a main-sequence donor which transfers mass via Roche-lobe overflow onto a White Dwarf (WD). DN experience quasi-regular, luminous outbursts during which accretion onto the WD proceeds at a high rate. Most of the time, however, DN are in quiescence, a phase during which the accretion rate onto the WD is much reduced (see Warner 1995 for a review).

¹Chandra Fellow

²Harvard Junior Fellow

Quiescent DN are well known sources of hard X-ray emission (Córdova & Mason 1983; Patterson & Raymond 1985a). This emission, typically at a level of $\sim 10^{30-32}$ erg s $^{-1}$, is consistent with Bremsstrahlung emission from a hot gas with temperatures $\sim 2 - 20$ keV (Patterson & Raymond 1985a; Eracleous, Halpern & Patterson 1991; Belloni et al. 1991; Yoshida, Inoue & Osaki 1992; Mukai & Shiokawa 1993). It has been commonly attributed to the boundary layer (BL) of the accreting WD, because at low enough accretion rates ($\lesssim 10^{16}$ g s $^{-1}$), the BL is unable to cool before it expands out of the plane of the accretion disk, so that it is hot, optically-thin and therefore a significant source of hard X-rays (Pringle & Savonije 1979; Tylenda 1981; King & Shaviv 1984; Patterson & Raymond 1985a).

Detailed calculations by Narayan & Popham (1993) show that the optically-thin BLs of accreting WDs are also radially extended (on the order of the WD radius in their models) and that they advect part of the internally dissipated energy inwards to the WD surface as a consequence of their inability to cool. The similarities between the optically-thin BL solutions of Narayan & Popham (1993) and ADAF solutions (Ichimaru 1977; Rees et al. 1982; Narayan & Yi 1994; 1995; Abramowicz et al. 1995; see Narayan, Mahadevan & Quataert 1998 for a review) prompted Menou (2000) to propose that ADAFs could actually be present around WDs accreting at low rates, such as in some quiescent DN.

ADAF models applied to accreting WDs are able to reproduce the typical X-ray luminosities of quiescent DN, as well as the range of plasma temperatures inferred from early X-ray observations. In addition, advection in the ADAF results in a large amount of energy deposited onto the central WD. If this energy is thermalized in the WD atmosphere before being radiated away, a strong EUV emission component originates from the heated atmosphere which can explain the luminous He II $\lambda 4686$ lines often observed in quiescent dwarf novae as being the result of disk irradiation (Menou 2000). In fact, the presence of such a component had been suggested by previous studies which emphasized the large supply of EUV photons (difficult to observe directly) required to explain the strength of the lines by photoionization of the disk material (Patterson & Raymond 1985b; Vrtilik et al. 1994). Simple BL models (in which one assumes the kinetic energy of the accreting gas just above the WD surface is radiated as isothermal, optically-thin Bremsstrahlung emission; e.g., Tylenda 1981; Patterson & Raymond 1985a) do not offer any satisfying explanation to the strength of these lines (see also, e.g., Ferland et al. (1982) for a discussion of additional difficulties faced by simple models).

The success of ADAF models applied to quiescent DN in providing an explanation for both the hard X-ray emission and the strong He II lines is attractive, but not compelling. In particular, X-ray eclipse observations indicate that a radially extended ADAF is not present in all quiescent DN (Wood et al. 1995; Mukai et al. 1997; Pratt et al. 1999; Menou 2000). In this paper, we emphasize that the presence of an ADAF can be tested in non-eclipsing systems by detecting (or not) thermal emission lines from the hot plasma, which are robust predictions of the theoretical models (Narayan & Raymond 1999). Line diagnostics can put severe constraints on the structure of the hot flow (Perna, Raymond & Narayan 2000); this is especially true for quiescent DN, which

are systems with a value of the WD mass and the inclination to the line of sight often relatively well constrained.

Other variations on the theme of a thin Shakura-Sunyaev (1973) disk with a hot, optically thin boundary layer include the model of King & Shaviv (1984), who emphasized the role of thermal conduction and the qualitative change expected at higher accretion rates. The optically thick boundary layers of high accretion rate systems produce less luminosity than expected from the outer disk luminosity (e.g., Mauche, Raymond & Mattei 1995; Popham & Narayan 1995) through some combination of advection and loss in a wind.

In §2, we recall some important properties of the DN SS Cyg to be used as constraints for the models. In §3, we describe the ADAF models and the numerical code used for the spectral predictions. In §4, we show predictions for the system SS Cyg and we emphasize the important constraints that can be put on the structure of the hot flow from detailed X-ray line diagnostics. Finally, we discuss some consequences and limitations of this work in §5, before summarizing our main results in §6.

2. SS Cygni and its quiescent X-ray emission

Observations show that some quiescent DN are more likely to harbor an ADAF than others. In particular, of the five DN observed in quiescence by the Hopkins Ultraviolet Telescope (Long 1996; spectral range $\sim 830 - 1860\text{\AA}$), three (WX Hyi, Yz Cnc and SS Cyg) show strong, blue continua with no evidence for the presence of a normal WD atmosphere (broad instead of narrow emission lines and no evidence for the expected broad $\text{Ly}\alpha$ absorption feature). These three sources are ideal candidates for the presence of an ADAF because a blue UV continuum is expected if the WD atmosphere is heated up to several 10,000 K by a substantial amount of energy advection in the surrounding hot flow (Menou 2000). SS Cyg is one of the best studied DN (see, e.g., Warner 1995), a bright source of X-ray emission in quiescence and is an approved target for observation with the *Chandra X-ray Observatory*. This motivates us to construct specific models for this system in what follows. The only other X-ray spectral models of SS Cyg in quiescence that we know of are the one-temperature models of Done & Osborne (1997), which are based on the BL solutions of Narayan & Popham (1993).

The mass of the WD in SS Cyg is $M_{\text{WD}} \simeq 1.2M_{\odot}$ and the inclination of the system to the line of sight is $i \simeq 40^{\circ}$ (Ritter & Kolb 1998). This inclination guarantees that the broadening of the X-ray lines from an ADAF is dominated by the bulk motion of the flow rather than thermal and turbulent motions (see below). The X-ray emission of SS Cyg during quiescence is variable. It has been characterized by an X-ray luminosity in the range $10^{31} - 10^{32} \text{ erg s}^{-1}$ (in various X-ray bands) and gas temperatures in the range 5 – 19 keV (see, e.g., Yoshida et al. 1992; Mukai & Shiokawa 1993).

3. Modeling techniques

There are a number of important assumptions made in the models presented below. For clarity, we briefly recall them here, while a more detailed discussion of these assumptions and their validity can be found in Menou (2000).

The hot flow structure used in the present study for the spectral calculations is nearly identical to the self-similar ADAF solutions described by Narayan & Yi (1994). This flow must make a transition from a large (but still subsonic) radial speed to a zero radial speed at the stellar surface. It is assumed that this transition happens in a narrow region (boundary layer, or BL) in the vicinity of the WD surface. The structure of this BL is not described in any detail here. The amount of mechanical energy released in this region (which depends on the stellar rotation rate) is comparable to the amount of energy radiated by the ADAF (Menou 2000). In all the models presented, we assume that both this mechanical energy and the much larger amount of energy advected by the ADAF (see below) are released at the WD surface as extreme-UV radiation,³ so that these additional components are not considered in the X-ray emission models presented (broadband models show that the EUV radiation goes to infinity without interacting significantly with the flow, though prominent HeII emission lines may be a signature of this component; Menou 2000). We expect a roughly blackbody spectrum with the luminosity of the advected energy from the WD surface, but detailed models of the fraction of the WD surface covered and of the structure of the heated atmosphere are needed to make more specific predictions.

3.1. ADAF models

The radial profiles of physical quantities in the hot flow, such as density, radial and azimuthal velocities and temperature are obtained from ADAF models and then used as an input for the detailed spectral calculations described in §3.2. We use two specific ADAF models presented by Menou (2000), which have parameters appropriate for SS Cyg: $M_{\text{WD}} = 1.2M_{\odot}$ (WD mass), $R_{\text{WD}} = 5 \times 10^8$ cm (WD radius), $\alpha_{\text{ADAF}} = 0.2$ (viscosity parameter), $\beta = 6$ (ratio of gas to magnetic pressure), $\gamma = 1.636$ (adiabatic index of the fluid, which includes contributions from the particles, the turbulence and the magnetic field; see Quataert & Narayan 1999), $\delta = 10^{-2}$ (fraction of direct electron viscous heating; unimportant for the present models), $p = 0$ (no wind) and $\dot{M} = 7 \times 10^{-3} \dot{M}_{\text{Edd}}$ (accretion rate), where $\dot{M}_{\text{Edd}} = 1.39 \times 10^{18} (M_{\text{WD}}/M_{\odot}) \text{ g s}^{-1}$ is the Eddington accretion rate for a 10% radiative efficiency. In the two models, this value of \dot{m} corresponds to a physical accretion rate $\dot{M} \simeq 10^{16} \text{ g s}^{-1} \simeq 1.5 \times 10^{-10} M_{\odot} \text{ yr}^{-1}$, a 0.5 – 10 keV X-ray luminosity of $\simeq 2 \times 10^{31} \text{ erg s}^{-1}$ and $\approx 85\%$ of the total gravitational energy liberated being advected by the flow.

³The large amount of energy advection results in significant heating of the WD and could have important consequences on the structure of its envelope (e.g. Shaviv & Starrfield 1987; Pringle 1988; Regev & Shara 1989)

The difference between the two models comes from the radial extent of the ADAF. In model I, the ADAF extends from the WD surface at R_{WD} up to $R_{\text{max}} = 10^4 R_s$, where $R_s = 3 \times 10^5 (M_{\text{WD}}/M_{\odot})$ cm is the Schwarzschild radius. In model II, the ADAF extends further out, up to $R_{\text{max}} = 10^5 R_s$. In addition, the accretion rate in the ADAF decreases as R_{trans}/R beyond $R_{\text{trans}} = 10^4 R_s$ in model II, to represent a corona accreting gas that is gradually being evaporated from an underlying thin disk (see Menou 2000 and Esin, McClintock & Narayan 1997 for details). In the following, we neglect the role, even indirect, that the disk could have on the X-ray spectrum emitted by the system (see §5 for a discussion of a possible reflection component). Except for the spectral calculations, all the other model characteristics are similar to those described in Menou (2000).

Panels (a) and (b) of Figure 1 show the radial profiles of various quantities in models I and II, respectively. At radii $\gtrsim 10^3 R_s$, the ions and the electrons in the ADAF have essentially the same temperature (because of an efficient coupling by Coulomb collisions), from a few 10^8 K close to the WD to $\sim 10^7$ K further away. This range of temperatures is ideal for the efficient production of thermal X-ray emission lines (Narayan & Raymond 1999). The radial profiles closely follow the self-similar ADAF solutions of Narayan & Yi (1994). A change in the slope of the density profile is clearly visible in Figure 1b; it corresponds to the radius R_{trans} beyond which the mass accretion rate in the ADAF starts decreasing with R . Figure 1 also shows that the azimuthal speed of the gas in the ADAF (or equivalently its angular rotation speed) is substantially sub-Keplerian ($\Omega \simeq 0.2\Omega_K$ in the present models).

3.2. Spectral models

We compute the X-ray spectra using an extended version of the Raymond & Smith (1977) code. The code computes the Bremsstrahlung, recombination and two-photon continua, as well as the emission in spectral lines. The effects of collisional excitations (see, e.g. Pradhan, Norcross & Hummer 1981 and Pradhan 1985), recombinations to excited levels of H-like and He-like ions (see, e.g., Mewe, Schrijver, & Sylwester 1980) and dielectronic recombination satellite lines (see, e.g. Dubau et al. 1981 and Bely-Daubau et al. 1982) are all included in the calculation. The ionization state of the elements is computed self-consistently within the code itself. Given the typical range of densities and infall velocities in the ADAF (see Fig. 1), the ionization time is much smaller than the infall time and the ionization state of the elements is very close to equilibrium. Note that in computing the expected luminosities, we do not take into account the partial obscuration by the central WD of the inner shells of the accretion flow. This should not strongly affect our predictions because the outer regions of the flow contribute significantly to the total luminosity in the radially extended ADAF models presented here. The high temperature regions close to the WD surface would be most strongly affected and the fluxes from these regions (which may be so hot that they do not contribute much to the line emission) would be reduced by a factor two at most.

Let $E_m(r, \theta)$ be the emissivity in a given line, and let v_{los} be the local component of the

velocity along the line of sight to the observer. The emission profile of a line as measured by an observer is then given by

$$\Phi(v) = \int_0^{2\pi} d\phi \int_0^\pi d\theta \sin\theta \int_{r_{\text{in}}}^{r_{\text{out}}} dr r^2 E_m(r, \theta) \Phi'(v; r, \theta, \phi) \quad \text{ergs s}^{-1} (\text{km s}^{-1})^{-1}, \quad (1)$$

where

$$\Phi'(v; r, \theta, \phi) = \frac{1}{\sqrt{\pi}\Delta} \exp \left\{ -\frac{[v - v_{\text{los}}(r, \theta, \phi)]^2}{\Delta^2} \right\}, \quad (2)$$

and $\Delta = \sqrt{2k_B T/m_a + v_{\text{turb}}^2}$ for an atom of mass m_a . For the turbulent velocity, we adopt $v_{\text{turb}} \simeq \alpha_{\text{ADAF}} c_s$, where $c_s = (\gamma \mu k_B T/m_p)^{1/2}$ is the fluid adiabatic sound speed and $\mu = 0.5$ its mean molecular weight. In the models presented below, we find that line broadening is largely dominated by the flow bulk motion, with only a small contribution from the turbulent motions (the contribution from the thermal motions is negligible for the heavy element X-ray lines discussed here; this also implies that turbulence is supersonic for the heaviest species).

4. Results

4.1. Continuum and Line Emission

Whereas the emission of thermal X-ray lines is a robust prediction of models of hot accretion flows, the detailed spectrum is not. It depends on several parameters of the model, such as the radial extent and the run of density in the hot flow. As we show below, this property can be used, in turn, to constrain the structure of the hot flow from detailed X-ray spectroscopic diagnostics.

The X-ray spectra corresponding to models I and II are shown in panels (a) and (b) of Figure 2. The spectra are characterized by emission lines of Fe, O, Si and other heavy elements, superposed on the Bremsstrahlung continuum. Note that a solar abundance has been assumed for the elements in the gas. Deviations from solar abundances could result in the lines of specific elements being weaker or stronger than in the models presented here. The shape of the continuum and line emission contains information on the structure of the hot flow. As a sum of the emission of shells of various densities ρ and temperatures T (see Fig. 1), a careful fit to an observational spectrum should provide valuable constraints on ρ and T in the hot flow. For instance, it is clear from Fig. 2 that there is additional low-energy Bremsstrahlung continuum emission in model II relative to model I, because of the additional emission from the outer and cooler regions of the flow.

The relative importance of the various lines in the spectrum is also indicative of the density, temperature and radial extent of the hot flow. For the ADAF models, lines formed at temperatures $\lesssim 10^8$ K are absent from the emission spectrum if the radial extent of the flow is $\lesssim 10^4 R_s$ (Fig. 2, panel a), while they become clearly apparent if the outer radius of the flow corresponds to a temperature $\sim 10^7$ K (model shown in Fig. 2, panel b). Similarly, in a model where the accretion

rate in the ADAF is not decreasing with radius beyond $R_{\text{trans}} = 10^4 R_s$ (like in model II), but is constant with radius, lines preferentially emitted at temperatures $\lesssim 10^8$ K would be stronger because of the higher densities in the outermost regions of the flow. This illustrates that the relative strengths of lines formed at various radii can be used to constrain the radial extent of the flow and its density profile⁴ (see Perna, Raymond & Narayan 2000 for details).

This can be complemented by measurements of line profiles, which strongly constrain the bulk motion of the hot gas in the flow. A crucial advantage that DN offer over other classes of systems that could harbor a hot flow is the (usually) relatively good knowledge of the mass (and therefore the size) of the accreting WD and of the inclination of the binary system. This provides an absolute scaling for the width of the emission lines, provided the line-of-sight velocities are known. Note that, except for small values of the inclination angle, broadening by the flow bulk motion is expected to dominate over thermal broadening for determining the width of the thermal X-ray lines in an ADAF.

Panels (a) and (b) of Figure 3 show the profiles of two strong lines, from iron and oxygen atoms respectively, for the inclination angle $i = 40^\circ$ of SS Cyg. The predicted width of the lines is $\lesssim 500 \text{ km s}^{-1}$. Note that the oxygen line is narrower than the iron line because it is produced in cooler regions of the ADAF, where it rotates more slowly. The width of these lines is a direct probe of the sub-Keplerian rotation in the hot flow because the inclination of the system (and to some extent the region of emission) is known. In particular, if the rotation rate of the flow were Keplerian, lines would be expected to be ~ 5 times broader. Since the sub-Keplerian rotation is due to partial radial pressure support by the hot gas, and this gas is hot because of energy advection, detection of these “narrow” lines would indicate the presence of energy advection in the flow.

4.2. Detectability with Current X-ray Instruments

At a distance of $\simeq 166$ pc (Harrison et al. 1999), the typical X-ray flux of SS Cyg (0.5–10 keV) is $10^{-11} \text{ erg cm}^{-2} \text{ s}^{-1}$ or more (Mukai & Shiokawa 1993). This allows a high quality spectrum to be taken in a few tens of ks of observation with the powerful X-ray satellites *Chandra* and *XMM-Newton*. The two satellites have spectroscopic instruments which approximately cover the soft and hard X-ray energy band corresponding to the spectra shown in Fig. 2. If a radially extended ADAF is present in SS Cyg, a spectrum taken by either of them should therefore yield valuable constraints on the general structure of the hot flow (radial extent, typical densities).

An important question is whether or not the width of the predicted lines (see Fig. 3) can be resolved by current instruments. The resolving power of the HETG on *Chandra* at 6.9 keV

⁴ Note that this can be done even for unknown elemental abundances, by considering lines from different ions of the same element.

is 200 (corresponding to 1500 km s^{-1}), which is of order 3 times the FWHM of the Fe XXVI line expected from the ADAF. This line cannot be resolved, but it should be possible, from a high quality spectrum, to rule out a line which is 5 times wider than predicted for the ADAF model. It should therefore be possible to test the Sub-Keplerian character of the hot flow with this instrument. Similarly, the resolving power of the HETG around 1 keV is 1000 (corresponding to 300 km s^{-1}), which is comparable to the width of the OVIII line expected from the ADAF. If such a line is detected at high enough S/N, it should be possible to tell with confidence if the hot emitting gas rotates at a substantially sub-Keplerian rate or not.

The two EPIC cameras onboard *XMM-Newton* have a resolving power of $\simeq 15$ at 1 keV and $\simeq 50$ at 6.4 keV, which is insufficient for the line diagnostics envisioned here. However, the RGS instrument (covering only the soft X-rays, from 0.35 to 2.5 keV) has a resolving power of $\simeq 300 - 500$ which should be sufficient to distinguish between a Keplerian and a substantially sub-Keplerian rotation rate. A possible advantage of RGS over the *Chandra* instruments is its larger sensitivity at low energies, allowing spectroscopy with higher time resolution.

5. Discussion

There is already evidence in the literature for X-ray line emission from DN in general and SS Cyg in particular. Mukai & Shiokawa (1993) find, from EXOSAT observations, that an emission line near 6.7 keV originates from many DN, including SS Cyg. Yoshida et al. (1992) find with the Ginga satellite that the X-ray emission of SS Cyg in quiescence shows an emission line around 6.68 keV (see also Done & Osborne 1997). These observations are therefore encouraging in suggesting the presence of a hot flow around the WD. Their quality, however, is insufficient to carry out the detailed spectroscopic diagnostics described above.

These diagnostics will become possible with the new powerful X-ray satellites *Chandra* & *XMM-Newton*. It should be possible, from high quality X-ray spectra, to discriminate between the case of accretion via an ADAF and the presence of a disk boundary layer (BL) in a quiescent DN. To our knowledge, there is no detailed spectral prediction for the emission originating from a compact BL (at low accretion rates), but one expects emission from a much denser gas than in the radially extended ADAF, possibly with temperatures ranging from the keV range all the way down to the WD atmospheric temperature at 15,000 K or so. In first approximation, the dissipation of the rotational kinetic energy of the gas in the boundary layer leads to temperatures T such that $3k_B T \sim 1/2 m_p (V_K^2 - V_*^2)$, where V_K is the Keplerian speed in the disk and V_* is the speed at the stellar surface. If T drops toward the WD surface, lines from cooler regions should have smaller rotational widths. For example, the model of Mahasena & Osaki (1999) does not treat the azimuthal velocity explicitly, but it predicts that most of the energy liberated in the boundary layer is transported to a dense region close to the WD surface and radiated away at intermediate temperatures. Because the radiating gas is the part of the BL closest to the stellar surface, its angular speed should be close to that of WD, and the line widths should be even smaller than in

the ADAF case. However, broadening by turbulent motions and the fact that detailed and more realistic calculations show that energy is radiated radially outward and advected radially inward in BLs (e.g. Narayan & Popham 1993; Popham & Narayan 1995; Godon, Regev & Shaviv 1995; Regev & Bertout 1995) could modify this simple picture quite substantially.

A possibly important difference between an ADAF model and simple BL models (in which all the kinetic energy of the accreting gas is radiated as one-temperature Bremsstrahlung emission and the role of advection is neglected; e.g. Patterson & Raymond 1985a) is in the ionization state of the gas, as manifested in the emission line equivalent widths. The fundamental difference is that only a small fraction of the accretion luminosity in the ADAF model emerges as fairly energetic X-rays, while most of the luminosity of such a simple boundary layer does. Thus photoionization may be significant and the ionization parameter higher in the simple BL model. Elements such as oxygen will be more highly ionized, with O VII and O VIII replaced by O IX. Thus the O VII $\lambda 22$ and O VIII $\lambda 19$ lines should be weaker in the simple BL model than in an ADAF model. In that respect, the models presented in this study (specific to SS Cyg) have general properties which are representative of what is expected from ADAFs possibly present in other quiescent DN. More specific BL model predictions for emission line fluxes and profiles are badly needed.

The spectral models presented in this study are for specific values of the ADAF model parameters (such as $\alpha_{\text{ADAF}} = 0.2$ and $\dot{M} = 7 \times 10^{-3} \dot{M}_{\text{Edd}} \simeq 1.5 \times 10^{-10} M_{\odot} \text{ yr}^{-1}$). We find, however, that the spectral predictions would be only marginally affected, or affected in trivial ways, if these parameters were changed, so that we felt it was unnecessary to explore here the parameter space of the ADAF models. For example, line profiles are sensitive to the value of α_{ADAF} only for small values of the inclination⁵, while line ratios are completely insensitive to changes in α_{ADAF} ⁶. Changes in the values of \dot{M} do affect the overall spectrum, by rescaling the overall continuum and line emission, but without relative changes between the lines. The rate of rotation, on the other hand, depends rather sensitively on the adiabatic index γ of the fluid. Note, however, that even if extreme values are assumed for this variable in an ADAF, the flow still remains sub-Keplerian ($\Omega \lesssim 0.5\Omega_{\text{K}}$ when $\gamma \rightarrow 4/3$; Narayan & Yi 1995) and our conclusions are mainly unchanged.

A possible ingredient of the X-ray spectrum of a quiescent DN that has been omitted from our calculations is the iron K_{α} fluorescence line at 6.4 keV from the X-ray irradiated disk. This line can appear on top of the Bremsstrahlung continuum emission, depending on the radial extent of the truncated disk. The width of the line, related to the Keplerian rotation rate in the inner regions of the disk and the system inclination is \sim a few 10 eV at most (Menou 2000). This is still narrow enough that the line should be easily separable, in a good quality spectrum, from the

⁵It is only the radial component of the flow velocity that depends on α , but not the rotational one. At small inclinations, turbulent motions become the main source of line broadening, together with thermal motions.

⁶The run of density is independent of α_{ADAF} (only the overall scaling depends on it), and the run of temperature does not directly depend on the value of α_{ADAF} (it depends only on the value of β ; see, e.g., Menou 2000).

other iron lines expected at 6.7 and 6.9 keV (from the hot gas).

Finally, it is important to notice that there are possible complications in interpreting narrow X-ray emission lines in terms of energy advection in a hot flow. One possible source of confusion comes from lines emitted in the close vicinity of the WD (for instance in a disk BL scenario), which is also likely to be rotating at a sub-Keplerian rate (see Sion 1999 for existing constraints on the rotation rate of WDs in DN). The sub-Keplerian rotation of the emitting gas can therefore be associated to the property of energy advection of the hot flow only if it can be shown that it is not directly related to the slow rotation of the WD. This may require clear evidence that the hot flow is indeed radially extended. We also note that Medvedev & Narayan (2000) recently presented solutions for accretion onto a compact object in which the flow can be radially extended and have a substantially sub-Keplerian rotation rate, without advecting any energy.⁷ If such a hot flow were present around WDs in quiescent DN, it could also be at the origin of narrow X-ray emission lines. The interpretation of narrow lines in terms of energy advection will therefore require some knowledge of other properties of the flow, such as its density profile, which differs in the ADAF solutions and the solutions of Medvedev & Narayan (2000). The knowledge of the WD rotation rate in some DN and the possibility of actually resolving some of the low energy X-ray lines predicted for ADAFs (§4.2) should provide critical observational tests of these two accretion scenarios.

6. Conclusion

We have constructed detailed spectral models of an ADAF around a WD, with model parameters appropriate for the Dwarf Nova SS Cygni in quiescence. The ADAF is a source of X-ray Bremsstrahlung continuum emission, which is characteristic of its density, temperature and radial extent.

Strong X-ray lines are also emitted by highly ionized atoms of Fe, O, Si and other heavy elements in the flow. The pattern of emission lines is a robust probe of the density, temperature and elemental abundances in the hot flow, which can therefore be constrained from high quality X-ray spectra.

In addition, the width of the X-ray emission lines can be directly related to the bulk motion of the gas in the ADAF by using the *a priori* knowledge of the mass of the WD and the inclination to the line of sight of the system. Current X-ray instruments have the capabilities to distinguish between lines emitted from a flow rotating at or substantially below the Keplerian rate. The property of energy advection of the flow, which is at the origin of the sub-Keplerian rotation in an ADAF, can therefore in principle be tested accurately by the observations.

⁷The rotation rate is directly related to that of the central object in these solutions.

Acknowledgments

We are grateful to Jonathan McDowell for many enlightening discussions on the observational capabilities of *Chandra*. Support for this work was provided by NASA through Chandra Postdoctoral Fellowship grant number PF9-10006 awarded by the Chandra X-ray Center, which is operated by the Smithsonian Astrophysical Observatory for NASA under contract NAS8-39073. Partial support was provided by NASA Grant NAG-528 to the Smithsonian Astrophysical Observatory.

REFERENCES

- Abramowicz, M.A., Chen, X., Kato, S., Lasota, J.-P. & Regev, O., 1995, *ApJ*, 438, L37.
- Belloni, T., et al., 1991, *A&A*, 246, L44.
- Bely-Daubau, F., Faucher, P., Dubau, J., & Gabriel, A. H. 1982, *MNRAS*, 198, 239
- Córdova, F.A. & Mason, K.O., 1983, in *Accretion Driven Stellar X-ray Sources*, eds. W.H. Lewin & E. van den Heuvel (CUP), p. 147.
- Done, C. & Osborne, J.P., 1997, *MNRAS*, 288, 649.
- Dubau, J., Loulergue, M., Gabriel, A. H., Steenman-Clark, L. & Volonte, S. 1981, *MNRAS*, 195, 705
- Eracleous, M., Halpern, J. & Patterson, J., 1991, *ApJ*, 382, 290.
- Esin, A.A., McClintock, J.E., & Narayan, R., 1997, *ApJ*, 489, 865.
- Ferland, G.J., Pepper, G.H., Langer, S.H., MacDonald, J., Truran, J.W. & Shaviv, G., 1982, *ApJ*, 262, L53.
- Godon, P., Regev, O. & Shaviv, G., 1995, *MNRAS*, 275, 1093.
- Harrison, T.E. et al., 1999, *ApJ*, 515, L93.
- Ichimaru, S., 1977, *ApJ*, 214, 840.
- King, A.R. & Shaviv, G., 1984, *Nature*, 308, 519.
- Kippenhahn, R. & Thomas, H.-C., 1978, *A&A*, 63, 265.
- Long, K., 1996, in *IAU Colloquium 158, “Cataclysmic Variables and Related Objects”*, Eds. A. Evans & J.H. Wood, p. 233.
- Mahasena, P. & Osaki, Y., 1999, *PASJ*, 51, 45.

- Mauche, C.W., Raymond, J.C. & Mattei, J.A., 1995, *ApJ*, 446, 842.
- Medvedev, M.V. & Narayan, R., 2000, *ApJ* submitted, *astro-ph/0007064*.
- Menou, K., 2000, *ApJ*, submitted, *astro-ph/0007185*.
- Meyer, F. & Meyer-Hofmeister, E., 1994, *A&A*, 288, 175.
- Mewe, R., Schrijver, J., & Sylwester, J. 1980, *A&AS*, 40, 323
- Mukai, K. & Shiokawa, K., 1993, *ApJ*, 418, 863.
- Mukai, K., Wood, Janet H., Naylor, T., Schlegel, E.M. & Swank, J.H., 1997, *ApJ*, 475, 812.
- Narayan, R., Mahadevan, R. & Quataert, E., 1998b, in *The Theory of Black Hole Accretion Discs*, eds. M. A. Abramowicz, G. Bjornsson, and J. E. Pringle (Cambridge: Cambridge University Press), *astro-ph/9803141*. Yi, I., 1996, *ApJ*, 457, 821.
- Narayan, R. & Popham, R., 1993, *Nature*, 362, 820.
- Narayan, R. & Raymond, J.C., 1999, *ApJL*, 515, L69.
- Narayan, R. & Yi, I., 1994, *ApJ Lett.*, 428, L13.
- Narayan, R. & Yi, I., 1995, *ApJ*, 444, 231.
- Patterson, J. & Raymond, J.C., 1985a, *ApJ*, 292, 535.
- Patterson, J. & Raymond, J.C., 1985b, *ApJ*, 292, 550.
- Perna, R., Raymond, J.C. & Narayan, R., 2000, *ApJ*, in press, *astro-ph/0005387*.
- Popham, R. & Narayan, R., 1995, *ApJ*, 442, 337.
- Pradhan, A. K. 1985, *ApJS*, 59, 183
- Pradhan, A. K., Norcross, D. W., & Hummer, D. G. 1981, *ApJ*, 246, 1031
- Pratt, G.W., Hassall, B.J.M., Naylor, T. & Wood, J.H., 1999, *MNRAS*, 307, 413.
- Pringle, J.E., 1988, *MNRAS*, 230, 587.
- Pringle, J.E. & Savonije, G.J., 1979, *MNRAS*, 187, 777.
- Quataert, E. & Narayan, R., 1999, *ApJ*, 516, 399.
- Raymond, J. & Smith, B. W. 1977, *ApJS*, 35, 419.
- Regev, O. & Bertout, C., 1995, *MNRAS*, 272, 71.

- Regev, O. & Shara, M.M., 1989, *ApJ*, 340, 1006.
- Rees, M.J., Phinney, E.S., Begelman, M.C. & Blandford, R.D., 1982, *Nature*, 295, 17.
- Ritter, H. & Kolb, U., *A&AS*, 129, 83.
- Shakura, N.I. & Sunyaev, R.A., 1973, *A&A*, 24, 337.
- Shaviv, G. & Starrfield, S., 1987, *ApJ*, 321, L51.
- Sion, E.M., 1999, *PASP*, 111, 532.
- Tylenda, R., 1981, *Acta Astr.*, 31, 267.
- Vrtilek, S.D., Silber, A., Raymond, J.C. & Patterson, J., 1994, *ApJ*, 425, 787.
- Warner, B., 1995, *Cataclysmic Variable Stars*, (Cambridge: Cambridge University Press).
- Wood, J.H., Naylor, T., Hassall, B.J.M. & Ramseyer, T.F., 1995, *MNRAS*, 273, 772.
- Yoshida, K., Inoue, H. & Osaki, Y., 1992, *PASJ*, 44, 537.

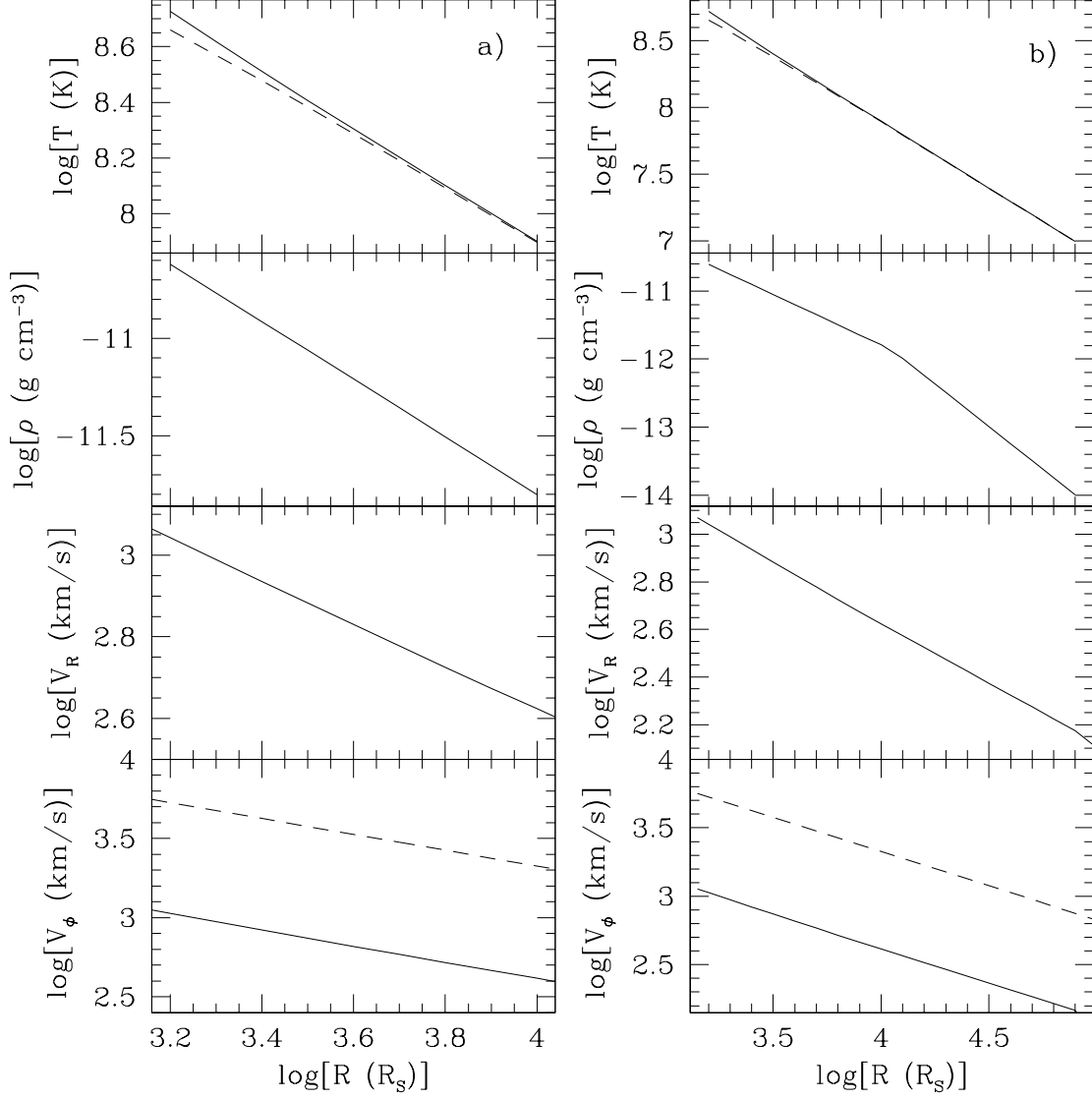


Fig. 1.— The radial profiles in ADAF models I (a) and II (b) of quantities that are important for the spectral calculations. From top to bottom, the panels show the gas temperature (solid: ions, dashed: electrons), the gas density, the radial infall speed and the azimuthal speed (solid: value for the ADAF, dashed: Keplerian value). Profiles are shown as a function of radius in Schwarzschild units, from $10^{3.15}$ ($= R_{WD} = 5 \times 10^8$ cm) to 10^4 ($\approx 7R_{WD}$) or 10^5 ($\approx 70R_{WD}$)

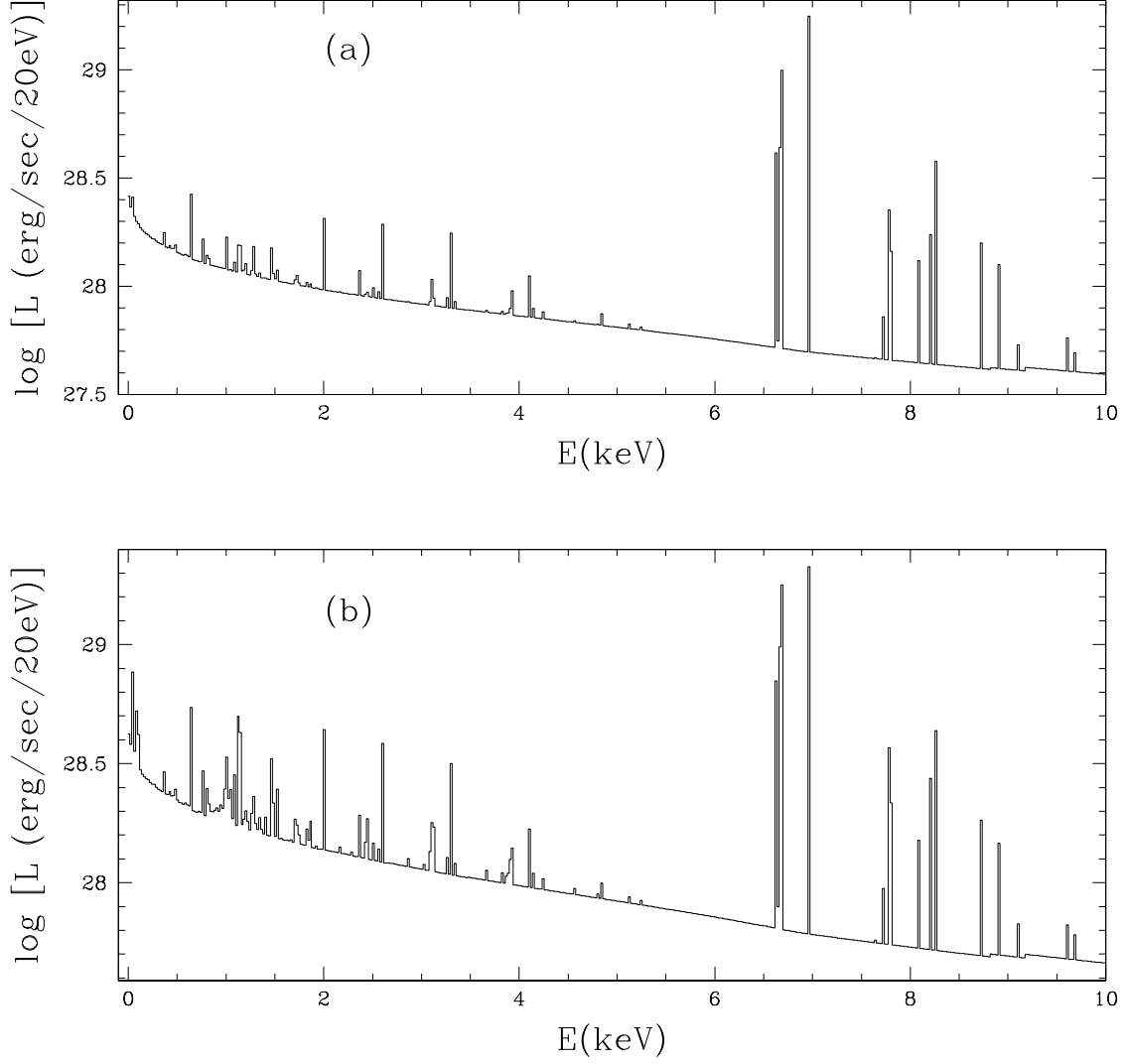


Fig. 2.— The predicted X-ray continuum and line emission for the ADAF models I (a) and II (b). In model II, the ADAF extends further out, where the gas is cooler and emits additional low-energy lines and Bremsstrahlung continuum. The various lines in (a) and (b) correspond to emission from atoms of Fe, O, Si and other heavy elements.

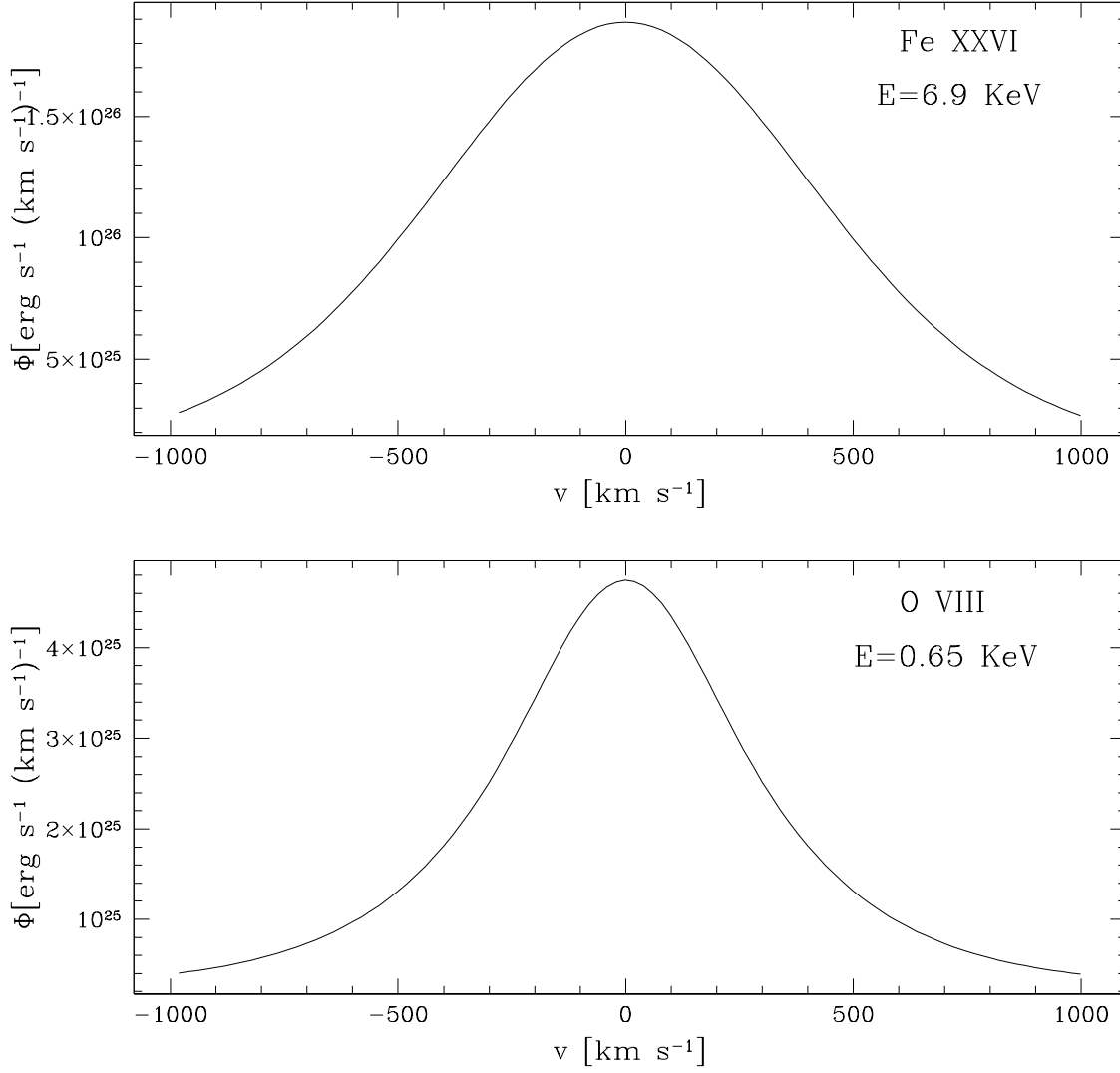


Fig. 3.— The predicted profiles for the strong iron line at 6.9 keV and the strong oxygen line at 0.65 keV in model II. The oxygen line is narrower than the iron line because it originates from cooler regions of the flow, where it rotates more slowly.